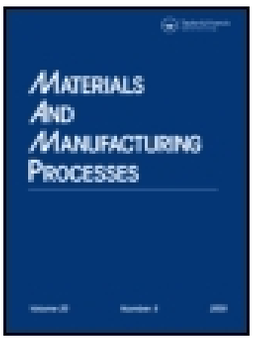

Materials and Manufacturing Processes

ISSN: 1042-6914 (Print) 1532-2475 (Online) Journal homepage: https://www.tandfonline.com/loi/lmmp20

Multi-objective optimization of the flat burnishing process for energy efficiency and surface characteristics

Trung-Thanh Nguyen, Le-Hai Cao, Xuan-Phuong Dang, Truong-An Nguyen & Quang-Hung Trinh

To cite this article: Trung-Thanh Nguyen, Le-Hai Cao, Xuan-Phuong Dang, Truong-An Nguyen & Quang-Hung Trinh (2019): Multi-objective optimization of the flat burnishing process for energy efficiency and surface characteristics, Materials and Manufacturing Processes, DOI: 10.1080/10426914.2019.1689266

To link to this article: https://doi.org/10.1080/10426914.2019.1689266

Published online: 11 Nov 2019.

MATERIALS AND MANUFACTURING PROCESSES
https://doi.org/10.1080/10426914.2019.1689266

Taylor & Francis
Taylor & Francis Group

Multi-objective optimization of the flat burnishing process for energy efficiency and surface characteristics

Trung-Thanh Nguyen [a,b], Le-Hai Cao[b], Xuan-Phuong Dang[c], Truong-An Nguyen[b], and Quang-Hung Trinh[b]

[a]Institute of Research and Development, Duy Tan University, Da Nang, Vietnam; [b]Faculty of Mechanical Engineering, Le Quy Don Technical University, Ha Noi, Viet Nam; [c]Faculty of Mechanical Engineering, Nha Trang University, Nha Trang, Viet Nam

ABSTRACT

The burnishing process is an impressive solution in order to improve the surface integrity. However, energy-efficient optimization of the burnishing process is rarely considered due to the high efforts required. This paper presented an input factor-based optimization to simultaneously enhance the power factor (PFB), the improvement of the Brinell hardness (K_{BH}), and the reduction of the average roughness (K_{Ra}), while energy consumption (ECB) aims to decrease for the burnishing process of SKD61 steel. The burnishing speed (*V*), the feed (*f*), and the depth of penetration (*d*) were considered as the processing factors. The trials were conducted using the matrix generated by Taguchi. The principal component analysis (PCA) was applied to calculate the weight values of responses. The optimal parameters were determined using the Technique for Order of Preference by Similarity to Ideal Solution (TOPSIS). The results showed that the optimal values of the *V*, *f*, and *d* are 700 RPM, 500 mm/min, and 0.13 mm, respectively. The technical outputs are primarily influenced by the feed rate and depth of penetration. The reductions of energy consumption and surface roughness are approximately 49.48% and 13.79%, while the power factor and Brinell hardness improve around 21.80% and 56.02%, respectively, as compared to the worst case.

ARTICLE HISTORY
Received 12 September 2019
Accepted 1 November 2019

KEYWORDS
Burnishing; power; factor; energy; surface; roughness; hardness; optimization; parameters

Introduction

Burnishing can be considered as an eco-green process to enhance the surface characteristics of machined components. The burnishing operations possess various attractive advantages, including decreased roughness, increased hardness, and generated compressive stress, which significantly contributes to improvements in mechanical properties, such as resistance and strength behaviors. Furthermore, this process can be used to decrease chip removal, tolerance affected, and performing knowledge of the machine, as compared to traditional finishing operations, such as grinding, honing, and lapping. Consequently, the burnishing operations are widely applied in the manufacturing of the different components having various surface kinds for industrial applications.

Many former researchers have performed the parameter-based optimizations in order to improve the technical responses of the different burnishing processes. The traditional objectives considered are the surface roughness, hardness, the hardened depth, and the residual stress. El-Taweel and Ebeid developed a new burnishing tool using an electrochemical part to enhance surface hardness and decrease the roundness deviation.[1] The outcomes revealed that the hardness was enhanced by 31.50% and 2.32 μm roundness deviation could be obtained. The response surface method (RSM) was applied in conjunction with the desirability approach to select the optimal parameters for improving the hardness and decrease the roughness for the ball burnishing process of hardened T215Cr12.[2] The optimized values of the roughness and hardness are 0.055 μm and 46.69 HRC, respectively. Travieso-Rodríguez *et al.* emphasized that the ball burnishing process has effective effects on the reduction in the roughness for concave and convex shapes.[3] The optimal values of the processing conditions were determined for the different treated materials. The impacts of the machining conditions on the surface properties for the burnishing processes of various EN steels were investigated by Babu *et al.*[4] The burnishing graphs were proposed to aid and achieve optimal factors. Revankar *et al.* indicated that the burnished surface's characteristics of titanium alloy were primarily affected by the *f*, *V*, and force (*F*), respectively.[5] The improvements in the roughness and hardness are 77% and 17%, respectively, as compared to the pre-machined conditions. Hamadache *et al.* concluded that the roughness and hardness of the burnished surface of 36 Cr Ni Mo 6 steel are 0.30 μm and 71.33 HRA at the optimal solution.[6] The technical responses were primarily influenced by the *F*, ball radius, and the number of the tool passes, respectively. Additionally, Cobanoglu and Ozturk stated that *f* and *F* have strong contributions to the surface's enhancements of AISI 1040 steel.[7] Moreover, the roughness was decreased by 50% and hardness was enhanced around 10%. The effects of the burnishing parameters on the surface properties, residual stress, and fatigue behavior of the burnished AISI 1010 steel were analyzed by Gharbi *et al.*[8] The

CONTACT Trung-Thanh Nguyen trungthanhk21@mta.edu.vn Faculty of Mechanical Engineering, Le Quy Don Technical University, 236 Hoang Quoc Viet, Ha Noi 100000, Viet Nam

Color versions of one or more of the figures in the article can be found online at www.tandfonline.com/lmmp.

reports revealed that the burnishing force caused an increment in the ductility and the compressive stress. A hybrid approach comprising the Taguchi and gray relational analysis was applied to improve the burnished surface's characteristics for the die material.[9] The authors stated that the enhancements in the roughness and hardness were 91% and 8 %, respectively when compared to the initial condition. The mathematical correlations of the roughness and hardness were developed in terms of the burnishing parameters using RSM.[10] The results indicated that the improvements of the roughness and hardness of the burnished titanium are around 63% and 28%, respectively, as compared to the pre-machined state. John *et al.* proposed the empirical formulations of the roughness and hardness with respect to the burnishing factors. The authors stated the burnished surface of EN-9 alloy has improvements in 94.50% and 41.70% for roughness and hardness, respectively.[11] Similarly, John *et al.* considered the impacts of the processing conditions on the dimensional and geometrical accuracy for the interior burnishing process.[12] The RSM models of the bore size, roughness, and ovality were developed in terms of the *V, f*, and the stock. The impacts of the process parameters, including the *V, f*, and *F* on the roughness, hardness, and corrosion resistance for the burnished carbon steel were analyzed.[13] The author stated that the roughness and hardness were improved by 83% and 14% with the optimal parameters, respectively. The outcomes revealed that the coated roller caused an increment in the hardness.

The RSM was used in conjunction with AMGA in order to decrease the roughness and improve the hardness as well as the depth of the affected layers for the internal roller burnishing.[14] The results indicated that the optimal values of the roughness, hardness, and the depth at optimized factors are 0.1 μm, 38.1 HRC, and 93.5 μm, respectively. Similarly, the optimal conditions were determined to improve surface integrity, including the roughness, hardness, and residual stress employing the Kriging models.[15] The author stated that the improvements in the roughness and hardness are 95.80% and 45.44%, respectively. Sachin *et al.* revealed that the surface roughness of 0.07 μm and hardness of 363 HV were achieved with the aid of a new tool having a diamond part.[16] The changes of the burnished surface morphology under different strategies were analyzed by Świrad *et al.*[17] The authors stated that the raster path is an appropriate solution in the burnishing of curved surfaces due to a lower roughness and stability. Huuki and Laakso emphasized that the ultrasonic burnishing is an effective solution to improve surface quality, as compared to the traditional approach.[18] Higher values of thickness of the affected layer and compressive residual stress could be obtained using a new machining approach. Amani *et al.* emphasized that the combination of the static and dynamic loading in the ultrasonic-assisted burnishing process effectively enhances the surface characteristics.[19] The hardness value and thickness of the affected layer were significantly improved at the optimal solution.

As a result, the common performances, including surface roughness and hardness were widely optimized to prove the machining efficiency of the burnishing processes. Furthermore, the burnished dimensions, geometrical deviation, the depth of affected layers, and the residual stress are rarely considered in the works published. The optimized factors are the burnishing speed, feed rate, depth of penetration, force or pressure, and the number of passes. However, the drawbacks of the papers published in terms of the burnishing processes can be listed as bellows:

The surface's characteristics, including the roughness, hardness, depth of affected layers, and residual stress were widely optimized in the aforementioned works. Unfortunately, the energetic parameters of the burnishing process, such as the power factor and energy consumption have not been presented in the papers published. The proper selection of process parameters significantly decreases energy consumption and enhances treated surface properties.

The selection of optimal factors for maximizing power factor, energy consumption, and surface properties for the burnishing process has not been thoroughly considered in the previous works. An urgent demand in industrial manufacturing is to decrease energy consumed, carbon emissions, and environmental impact due to the depletion of natural resources and rising energy costs. Consequently, improving the energy efficiency of the burnishing process is a necessary requirement to achieve greener manufacturing, reduction in carbon emissions, and saving environment.

This work presents a factor-based optimization for the flat roller burnishing process of mold material in order to enhance the power factor, the improvement of the Brinell hardness, and the reduction of the average roughness, while the energy consumption aims to decrease. An integrative approach comprising the Taguchi, principal component analysis (PCA), and TOPSIS is used to calculate the weight values and predict optimal factors.

Materials and methods

In this paper, four technical parameters, including the power factor, energy consumption, and the improvement of the Brinell hardness, and the reduction of the average roughness are simultaneously optimized.

The power factor of the burnishing process (PFB) is calculated as:

$$PFB = \frac{AP}{APP} = \frac{AP}{\sqrt{AP^2 + RP^2}} \quad (1)$$

where, AP, RP, and APP denote the active power consumption, the reactive power, and the apparent power, respectively. The apparent power is the vector sum of the active power and reactive power. The active power is a significant power, which is used to perform the useful load of the device. The reactive power is a useless power but it is necessary for energy conversion. A higher value of the power factor has a significant contribution to an improvement in active power; hence, the device will produce more useful power.

The variations of the power factor depend on the load of the electrical device. Practically, the modifications of operating conditions, such as spindle speed, feed rate, and material hardness may lead to the variable loads; hence, the power consumed and power factor changes. Therefore, the selection

of appropriate conditions is for enhancing the power factor is a significant approach and an important research.

The average value of the power factor in the burnishing time is calculated using Eq. 2.

$$PFB = \frac{1}{n}\sum_{i=1}^{n} PFB_i \tag{2}$$

where PFB_i and n are the power factor at the i position and the total measured point, respectively.

The total energy consumption of the burnishing process can be divided into two primary elements, including direct and indirect energy. The direct energy is consumed to perform the operational functions of the machine's components. The indirect energy is related to the embodied energy of burnishing tools and the fluid.

The direct energy consumption of the burnishing process can be classified into five components, including start-up energy, standby energy, air-burnishing energy, burnishing energy, and the energy of tool change. In practice, energy consumption for the start-up, standby, air-burnishing, and tool change stages are usually considered as constant values. Therefore, energy consumption in the burnishing time (ECB) is treated as an objective, which is used to produce the burnished surface. The value of the ECB is calculated using Eq. 3.

$$ECB = PCM \times t_b \tag{3}$$

where PCM and t_b denote the power consumed by machine and burnishing time, respectively.

The average value of the Brill hardness of the affected layer is taken from five positions. The improvement of the hardness (K_{BH}) is calculated by applying Eq. 4.

$$K_{BH} = \frac{ABH_B - ABH_{\mathrm{Pr}}}{ABH_{\mathrm{Pr}}} \tag{4}$$

where ABH_B and ABH_{Pr} are the average Brill hardness of the burnished and pre-machined surfaces, respectively.

The average values of the R_a are calculated at five different positions in the x and y directions. The reduction of the roughness (K_{Ra}) is calculated as:

$$K_{Ra} = \frac{R_{a\,\mathrm{Pr}} - R_{aB}}{R_{a\,\mathrm{Pr}}} \tag{5}$$

where R_{aB} and R_{aPr} are the average roughness of the burnished and pre-machined surfaces, respectively.

The process parameters are the burnishing speed (V), feed rate (f), and depth of penetration (d). Their values are shown in Table 1. The parameter ranges are determined based on the tool characteristics and material properties. The assigned levels have also matched the values used in the industrial burnishing process for molding plates. Furthermore, the experimental trials are performed using the lowest and highest levels to ensure the machinability of the specimens.

Table 1. Processing conditions.

Symbol	Parameters	Level 1	level 2	level 3	level 4
V	Burnishing speed (RPM)	400	700	1000	1300
f	Feed rate (mm/min)	200	350	500	650
d	Depth of penetration (mm)	0.04	0.07	0.10	0.13

The optimizing procedure having a multi-objective optimization method is shown in Fig. 1. The sequential steps are listed as bellows:

Step 1: A set of the burnishing trails is performed according to the Taguchi matrix to obtain the experimental data.[20]

Step 2: Normalization of the experimental data. The values of the responses are normalized using Eq. 6.

$$r_{ij} = \frac{q_{ij}}{\sqrt{\sum_{i=1}^{n} {q_{ij}}^2}} \tag{6}$$

where q_{ij} and r_{ij} represent the actual and normalized values of the response, respectively.

Step 3: Determining the weight values of performances using the PCA.

The PCA is used to prevent the subjective judgment and calculate the weight values of the technological responses. The correlation coefficient from the gray relation coefficient (GRC) is calculated by means of Eq.7:

$$R_{jl} = \left[\frac{Cov(x_i(j), x_i(l))}{\sigma x_i(j) * \sigma x_i(l)}\right], j = 1, 2, \ \ldots \ m, \ l = 1, \ 2, \ \ldots \ n \tag{7}$$

where $x_i(j)$ and $cov(x_i(j),x_i(l))$ are the gray relation coefficient and the covariance of the response. Additionally, $\sigma x_i(j)$ and $\sigma x_i(l)$ are the standard deviations of the response. The eigenvalues and consequent eigenvectors are determined using Eq. 8.

$$(R - \lambda_k I_m) V_{ik} = 0 \tag{8}$$

where λ_k, V_{ik}, and I_m represent the eigenvalues, the eigenvectors, and the identity matrix, respectively. Therefore, the principal components are obtained by means of Eq. 9.

$$Ymk = \sum_{i=1}^{n} x_m(i) V_{ik} \tag{9}$$

where $x_m(i)$ and Y_{mk} are the normalized response and the principal component, respectively.

Step 4: Determining the optimal parameter setting using the TOPSIS.[21]

The weighted value of the response is calculated based on the normalized value and the weight factor obtained by PCA, as shown in Eq. 10.

$$U_{ij} = r_{ij} w_i \tag{10}$$

The positive ideal solution (D^+) and the negative ideal solution (D^-) are determined as bellows:

$$U^+ = (v_1^+, v_2^+, v_3^+ \ldots, v_n^+) \text{ maximumvalues} \tag{11}$$

$$U^- = (v_1^-, v_2^-, v_3^- \ldots, v_n^-) \text{ minimumvalues} \tag{12}$$

$$D_i^+ = \sqrt{\sum_{j=1}^{m} (u_{ij} - u_j^+)^2} \tag{13}$$

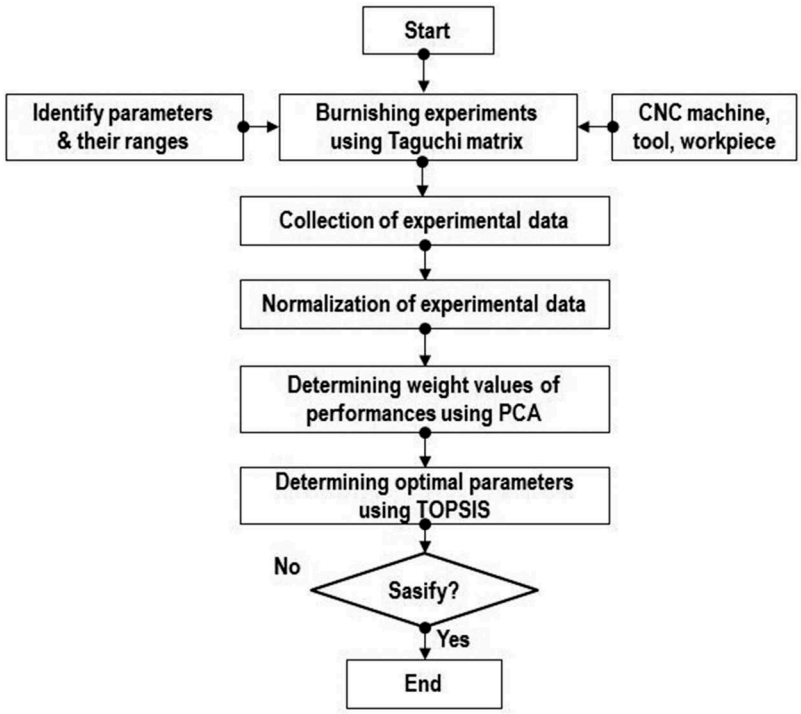

Figure 1. Optimization method.

$$D_i^- = \sqrt{\sum_{j=1}^{m} (u_{ij} - u_j^-)^2} \tag{14}$$

The best solution is observed with the highest value of the relative closeness (D_i):

$$D_i = \frac{D_i^-}{D_i^+ + D_i^-} \tag{15}$$

The burnishing trials are performed with the aid of a vertical machining machine. The burnishing tool having three hardened rollers is used to yield the treated surface. The burnishing workpiece has 60 mm length, 20 mm width, and 10 mm thickness. The workpiece is clamped on the precision vector vise. Commercial software entitled Master Cam is applied to generated the burnishing path. The numerical controlled (NC) program generated by the post-processor is transferred to the machine controller (Fig. 2a).

The power factor and power consumption in the burnishing process are measured using a power meter entitled KEW6305 (Fig. 2b). The experimental data are automatically recorded and stored in the device in the burnishing time. The offline software is used to visualize the obtained data on the computer monitor. The burnished specimens are shown in Fig. 2c.

The average value of the roughness is detected and calculated at five measured points with the aid of Mitutoyo SJ-301 (Fig. 2d). The values of the ABH_B are measured using a hardness tester entitled ERNST AT200 DR-TM. A test load of 3000 N is applied on the burnished surface in 15 seconds with the support of a testing ball.

The experimental results of the burnishing trials are exhibited in Table 2. The variations of the power factor in terms of the processing time are shown in Fig. 3. The values of the power consumed at the different inputs are depicted in Fig. 4. The roughness values of the burnished surfaces are shown in Fig. 5. The representative outputs of the Brinell hardness are exhibited in Fig. 6.

Results and discussions

The impacts of the process parameters on the power factor (PFB) are shown in Fig. 7. It can be stated that an increment in the input causes a higher value of the power factor. When the burnishing speed increases, higher power used of the motor is required to reach the targeted value of the rotational spindle. Therefore, the active power enhances and a higher power factor is obtained. At a higher value of the burnishing feed, the speed of the feed drive increases, this causes higher active power of the feed drive motors. As a result, PFB enhances. An increased depth of penetration leads to an increment in the burnishing pressure on the workpiece surface and the amount of the burnished material increases. The higher the burnishing pressure, the higher the material deformation and the higher active power is required to overcome the resistance. This leads to an increment in the power factor.

Figure 8 signifies the interactive effects between the inputs in affecting the power factor. The contribution of each factor on the power factor is shown in Table 3. As a result, the feed rate is the most significant factor with a contribution of 40.85%, followed by the depth of penetration (contributing 36.63%) and burnishing speed (contributing 20.52%), respectively. The feed has more effect on the PFB than that of the burnishing speed due to the contribution of the active power of the feed drive motors. When the feed rate increases, the reaction forces on the X and Y-axis of the feed drive system as well as the burnishing momentum on

(a) Burnishing experiment (b) Measuring power

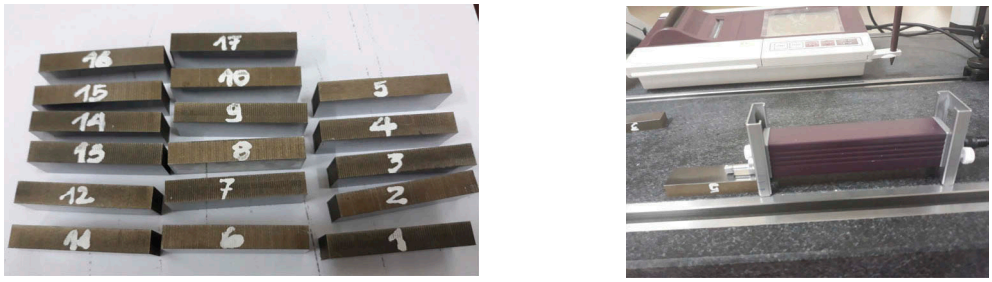

(c) Burnished specimens (d) Measuring roughness

Figure 2. Burnishing experiments and measurements.

Table 2. Experimental results.

No.	V (RPM)	f (mm/min)	d (mm)	PFB	ECB (kJ)	R_{aB} (μm)	K_{Ra}	ABH_B (HB)	K_{BH}
1	400	200	0.04	0.637	39.08	0.31	0.78	286	0.12
2	400	350	0.07	0.676	25.12	0.35	0.76	353	0.38
3	400	500	0.10	0.748	19.15	0.41	0.71	413	0.62
4	400	650	0.13	0.845	15.90	0.43	0.70	547	1.15
5	700	200	0.07	0.679	42.00	0.29	0.80	332	0.30
6	700	350	0.04	0.683	24.56	0.37	0.74	375	0.47
7	700	500	0.13	0.827	21.22	0.25	0.82	518	1.03
8	700	650	0.10	0.830	16.13	0.39	0.73	494	0.94
9	1000	200	0.10	0.735	45.99	0.21	0.85	406	0.59
10	1000	350	0.13	0.810	29.76	0.18	0.88	501	0.97
11	1000	500	0.04	0.740	18.76	0.46	0.68	423	0.66
12	1000	650	0.07	0.813	16.05	0.51	0.64	481	0.89
13	1300	200	0.13	0.815	49.12	0.23	0.84	507	0.99
14	1300	350	0.10	0.803	28.75	0.33	0.77	450	0.77
15	1300	500	0.07	0.808	20.24	0.49	0.66	475	0.86
16	1300	650	0.04	0.819	15.78	0.53	0.63	530	1.08

the spindle motor increases. Therefore, the total active power of the movement system increases.

The mean impacts of the processing conditions on energy consumption are shown in Fig. 9. As depicted, the ECB increases when the V increases from 400 RPM to 1300 RPM and the d changes from 0.4 mm to 1.3 mm. Moreover, the ECB significantly decreases when the f increases from 200 mm/min to 650 mm/min. At a higher value of the burnishing speed, more power is required to increase it from the rest to the desired value. The load of the spindle motor increases; hence, energy consumption eventually increases. When the feed rate increases, the reaction forces on the X and Y-axis of the feed drive system increase. Therefore, the total active power of the movement system increases. Obviously, higher power consumed is required to process material. Fortunately, a higher value of the feed rate leads to a decrease in the processing time, resulting in a reduction in the energy consumed. Reduction in energy consumption with an increase in burnishing feed is acceptable due to a faster burnishing and smaller processing time. An increment in the burnishing depth causes an increased contact area between the roller and workpiece. Consequently, more material burnished results in larger plastic deformation, leading to greater resistance in the burnished surface; hence, higher energy is consumed.

Figure 10 shows the interactions of the processing inputs in affecting energy consumption. Table 4 illustrates the contributions of the inputs, which have a significant impact on the ECB. As a result, the f is the major influencing factor due to the highest contribution of 95.28%, followed by d (2.34%), and V (1.68%).

Figure 11 clearly exhibits that the spindle speed, feed rate, and depth of penetration have significant impacts on the K_{Ra}. When burnishing speed increases, the temperature in the burnishing area enhances, leading to a reduction in the workpiece hardness. The material easily is processed from the peaks into valleys, resulting in a decreased roughness or an

(a) PFB at the V = 400 (RPM), f = 200 (mm/min), and d = 0.04 (mm)

(b) PFB at the V = 1000 (RPM), f = 200 (mm/min), and d = 0.10 (mm)

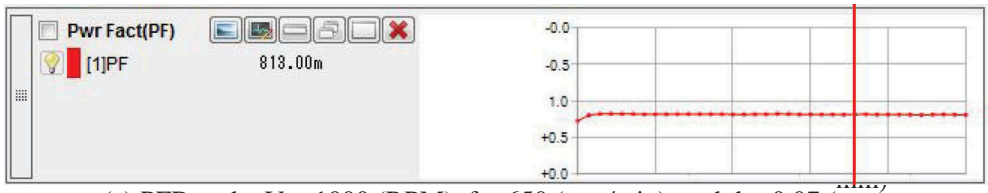

(c) PFB at the V = 1000 (RPM), f = 650 (mm/min), and d = 0.07 (

Figure 3. The power factor at the different inputs.

(a) PCM at the V = 700 (RPM), f = 350 (mm/min), and d = 0.04 (mm)

(b) PCM at the V = 400 (RPM), f = 650 (mm/min), and d = 0.1 (mm)

(c) PCM at the V = 1300 (RPM), f = 200 (mm/min), and d = 0.13 (mm)

Figure 4. The power consumption (PCM) at the different inputs.

enhanced K_{Ra}. In contrast, at an excessive speed, the machine requires more power consumed, which may lead to a vibration of the system. A higher roughness is observed due to the instability, results in a reduction in the K_{Ra}. As the feed rate increases, the distance between two adjacent burnishing traces increases. Moreover, higher burnishing forces, as well as, a machining instability will occur at an increased feed; hence, a higher roughness or a lower K_{Ra} is produced. As the burnishing depth increases, a higher burnishing pressure is produced on the machined surface. Obviously, the valleys are filled and a lower roughness is obtained. Consequently, an increased depth of penetration significantly contributes to improved K_{Ra}.

The interactive effects of the machining parameters on the reduction of the average roughness are depicted in Fig. 12. Table 5 shows the contributions of the inputs for the K_{Ra}. As a result, *f* has the largest contribution (59.38%), followed by *d* (33.01%), and *V* (7.16%), respectively.

The influences of the inputs on the K_{BH} are shown in Fig. 13. As a result, the K_{BH} is improved with an increased *V, f,* and *d*. It is seen from Fig. 13 that an increase in the speed from 400 RPM to 1300 RPM, the Brinell hardness impressively increases. An increased burnishing speed leads to an increment in the degree of the plastic deformation, which causes the work-hardening behavior; hence, the hardness enhances. Similarly, the degree of work hardening increases at a higher value of the speed, resulting in an improved hardness. At a higher value of the depth of penetration, the burnishing pressure increases and more material is pressed on the treated surface. Therefore, higher hardness is obtained. Generally, at a higher value of the input, excessive plastic deformation is observed, leading to work-hardening behavior. Therefore, the hardness of the affected layer is increased.

The interactive effects of machining parameters on the K_{BH} are shown in Fig. 14. Table 6 presents the factor's

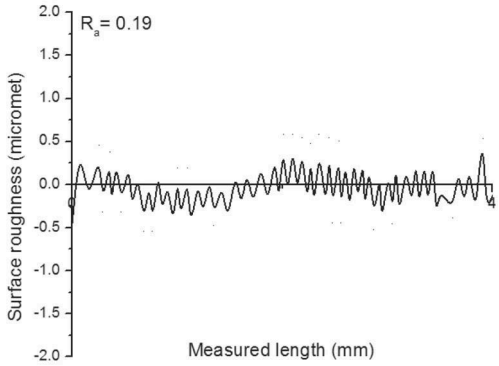

(a) R_{aB} at the V = 1000 (RPM), f = 350 (mm/min), and d = 0.13 (mm) (Rep. 2)

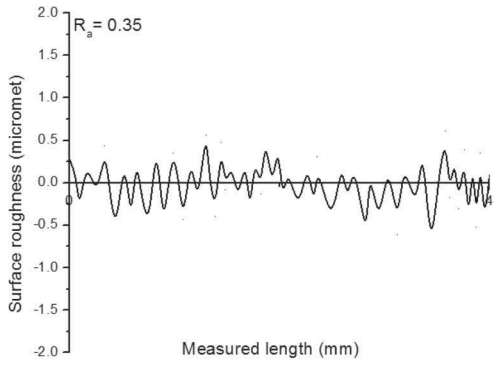

(b) R_{aB} at the V = 700 (RPM), f = 350 (mm/min), and d = 0.04 (mm) (Rep. 3)

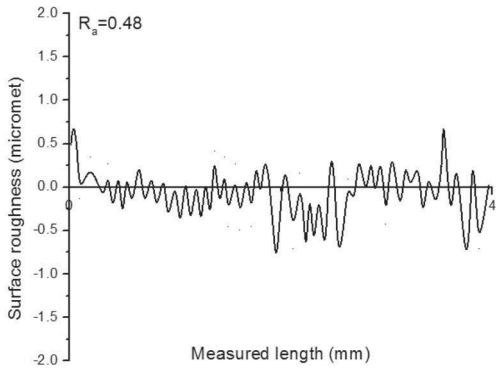

(c) R_{aB} at the V = 1300 (RPM), f = 500 (mm/min), and d = 0.07 (mm) (Rep. 3)

Figure 5. The surface roughness at different inputs.

(a) ABH_B at the V = 1000 (RPM), f = 500 (mm/min), and d = 0.04 (mm) (Rep. 2)

(b) ABH_B at the V = 1000 (RPM), f = 350 (mm/min), and d = 0.13 (mm) (Rep. 3)

(c) ABH_B at the V = 400 (RPM), f = 500 (mm/min), and d = 0.10 (mm) (Rep. 3)

Figure 6. The Brinell hardness at the different inputs.

contributions to the K_{BH}. As a result, the percentage contributions of the *f*, *d*, and *V* are 42.28%, 37.75%, and 19.97%, respectively.

The treated surface at various conditions is depicted in Fig. 15. As a result, the surface roughness effectively is decreased with the aid of the burnishing process.

The pre-processing and corresponding values for three objectives after a linear normalization are listed in Table 7. As depicted in Table 8, the percentage contribution of the first principal component is 75.00%, followed by the second component (23.50%), the third component (1.10%), and the fourth component (0.40%). The weight values are calculated

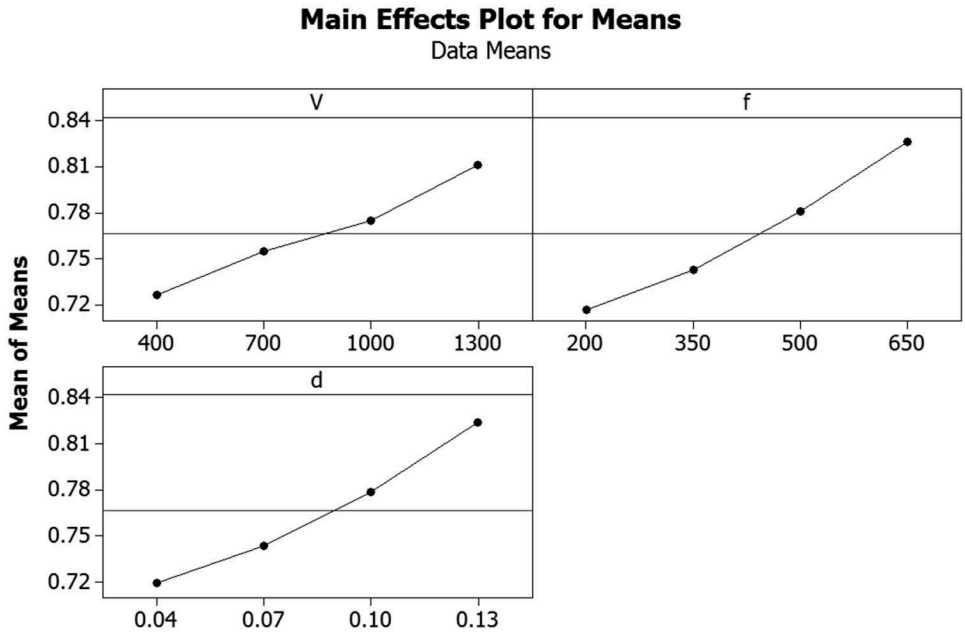

Figure 7. The main effects of machining parameters on the PFB.

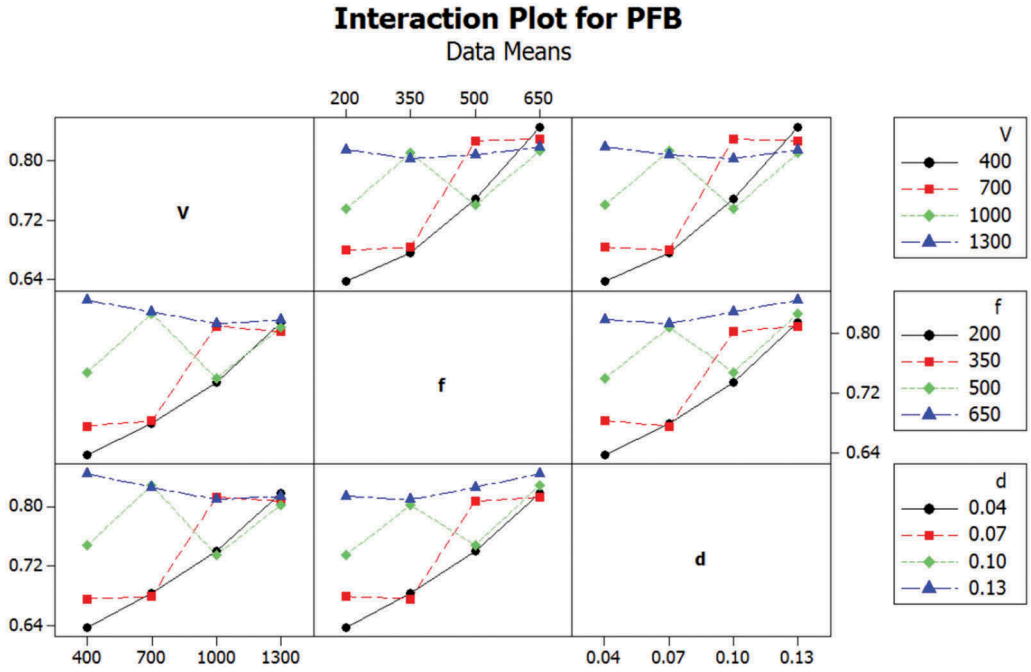

Figure 8. The interactive effects of machining parameters on the PFB.

Table 3. ANOVA results for the power factor.

Source	DF	Seq SS	Adj SS	Adj MS	F	P	Contribution
V	3	0.0151552	0.0151552	0.0050517	143.12	<0.0001	22.52
f	3	0.0274922	0.0274922	0.0091641	259.62	<0.0001	40.85
d	3	0.0246516	0.0246516	0.0082172	232.79	<0.0001	36.63
Error	6	0.0002118	0.0002118	0.0000353			
Total	15	0.0675108					

based on the squares of subsequent eigenvectors of the first and second components. Table 9 revealed that the weight value of the K_{Ra} is 0.28, followed by the PFB (0.25), K_{BH} (0.24), and ECB (0.23), respectively.

The normalized weighted values are shown in Table 10. The values of the positive and negative values are shown in Table 11. As a result, the highest D_i is observed at experimental No. 7, as listed in Table 11. The optimal values of the

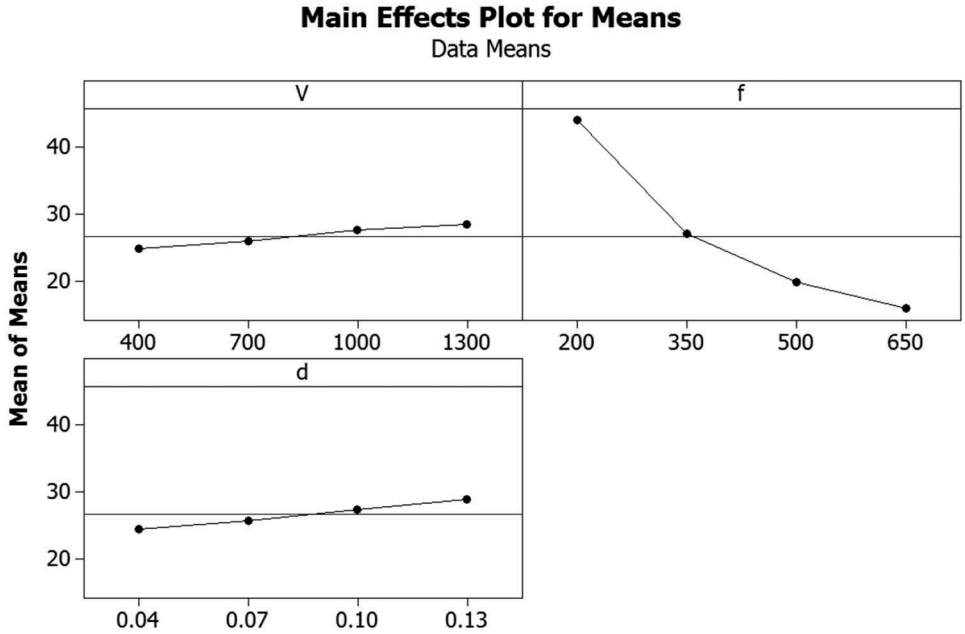

Figure 9. The main effects of machining parameters on the ECB.

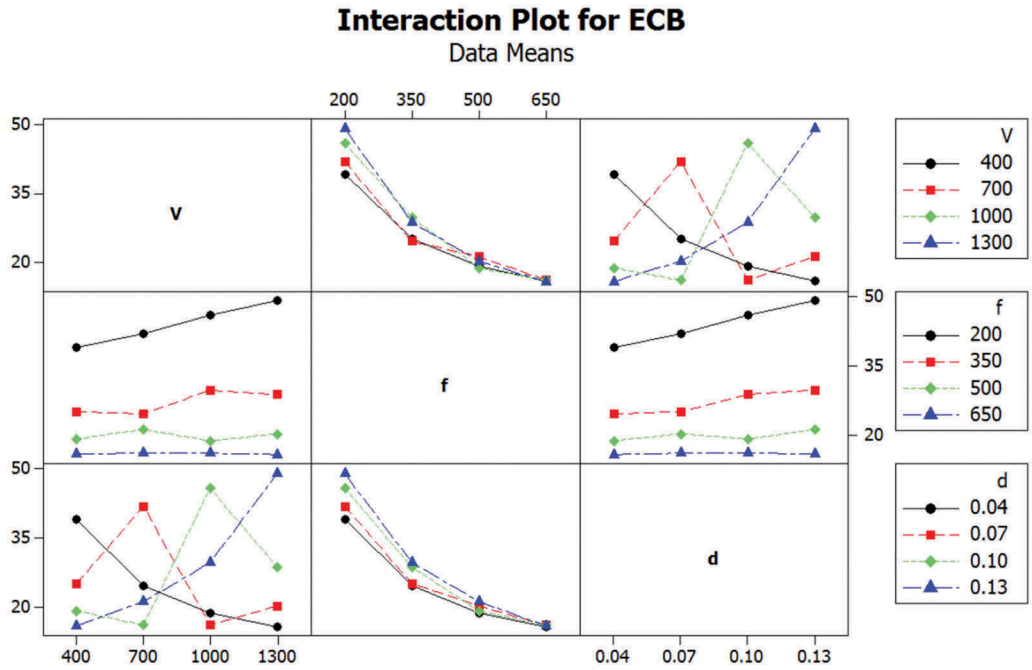

Figure 10. The interactive effects of machining parameters on the ECB.

Table 4. ANOVA results for energy consumption.

Source	DF	Seq SS	Adj SS	Adj MS	F	P	Contribution
V	3	32.43	32.43	10.81	13.83	<0.004	1.68
f	3	1853.28	1853.28	617.76	790.24	<0.0001	95.98
d	3	45.19	45.19	15.06	19.27	<0.002	2.34
Error	6	4.69	4.69	0.78			
Total	15	1935.59					

V, *f*, and *d* are 700 RPM, 500 mm/min, and 0.13 mm, respectively (Table 12). The power factor, the reduction of the average roughness, and the improvement of Brinell hardness are enhanced by 21.80%, 2.5%, and 243.33%, respectively at the optimal point, as compared to the worst-case (experimental No. 5). Energy consumption is significantly decreased by 49. 48%. The surface roughness is reduced by around 13.79% and the Brinell hardness is improved by 56.02%.

Recently, the reductions of energy used, carbon emissions, environmental impacts have become urgent needs of manufacturers. The industrial sector accounts for around 21% of total greenhouse gas emissions and more than 65% of gas emissions are carbon dioxide (CO2).[22] The electricity need of the world reaches to more than 23 000 TWh, leads to an increase in 33.1 Gt of CO2 emissions in 2018.[23] Although the improvements in fossil fuels, solar, and wind energy are

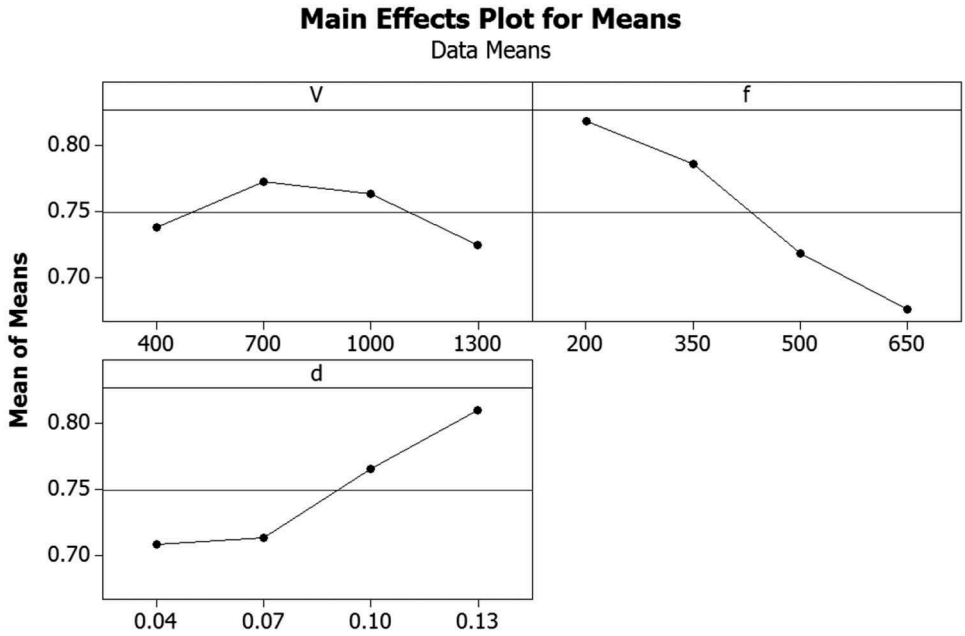

Figure 11. The main effects of machining parameters on the $K_{Ra.}$

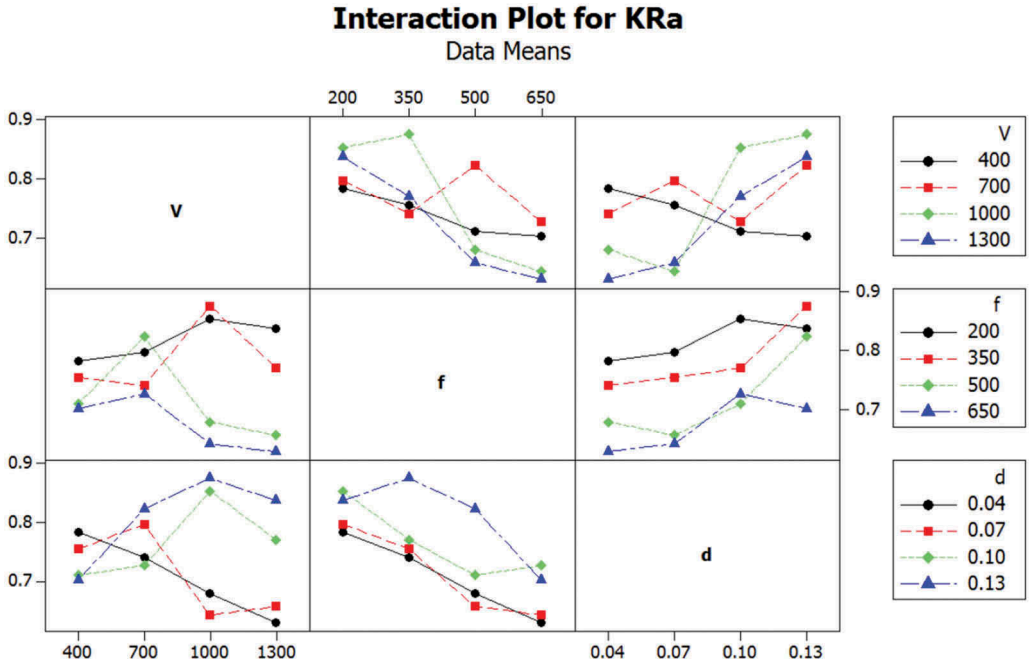

Figure 12. The interactive effects of machining parameters on the $K_{Ra.}$

Table 5. ANOVA results for the reduction of average roughness.

Source	DF	Seq SS	Adj SS	Adj MS	F	P	Contribution
V	3	0.0060030	0.0060030	0.0020010	3.10	0.001	7.16
f	3	0.0501506	0.0501506	0.0167169	25.90	<0.0001	59.83
d	3	0.0276751	0.0276751	0.0092250	14.29	<0.0001	33.01
Error	6	0.0038728	0.0038728	0.0006455			
Total	15	0.0877015					

approximately 70%, 31%, and 9.1%, the electrical requirement of the world is not comprehensive satisfy. The worldwide energy consumption will grow by 28% between 2015 and 2040.[24] In fact, an increase in energy consumption leads to the increased prices of all fuels and higher production costs are required.

For the burnishing operation, machine tools, the workpiece, the tools, and the fluid have negative effects on energy

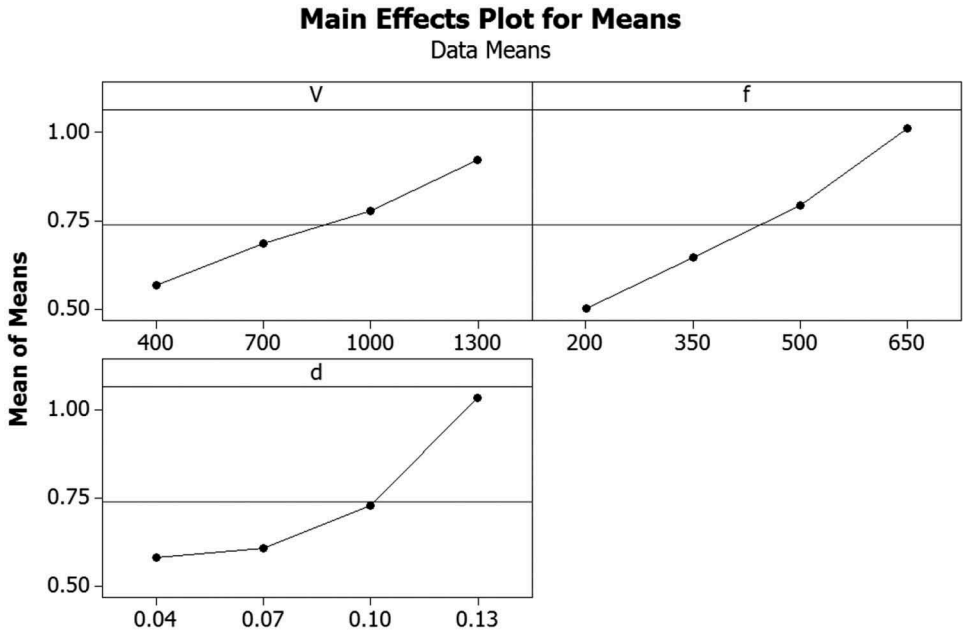

Figure 13. The main effects of machining parameters on the $K_{MH.}$

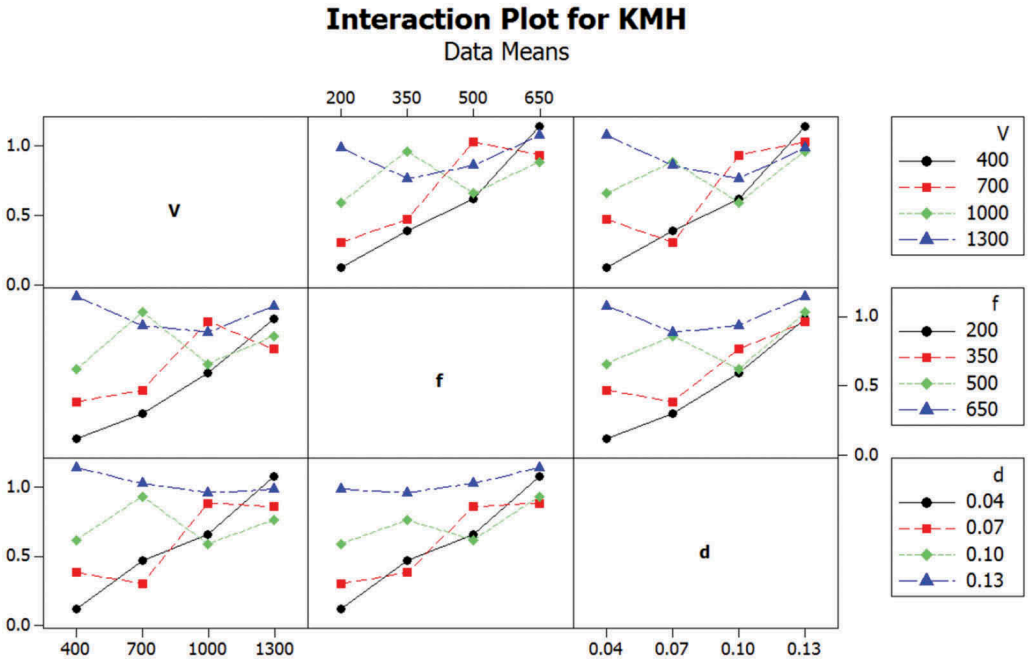

Figure 14. The interactive effects of machining parameters on the $K_{MH.}$

Table 6. ANOVA results for the improvement of Brinell hardness.

Source	DF	Seq SS	Adj SS	Adj MS	F	P	Contribution
V	3	0.27030	0.27030	0.09010	33.50	0.001	19.97
f	3	0.57213	0.57213	0.19071	70.91	<0.0001	42.28
d	3	0.51081	0.51081	0.17027	63.31	<0.0001	37.75
Error	6	0.01614	0.01614	0.00269			
Total	15	1.36938					

consumption and carbon emissions. Machine tools are the primary devices of industrial operations and they consume a large amount of raw materials and electrical energy during the processing time. Additionally, during the burnishing process, the tool and fluid are used to conduct the machining process. The production process of these factors consumes a large amount of embodied energy. An increment in these consumption leads to a serious issue of sustainable development and environmental protection. The outcomes of the investigated work result in a reduction in power consumption, resource exhaustion, and carbon emissions. Moreover, the results are expected as an effective contribution to make the flat burnishing process become greener and more efficiency.

In this paper, the process parameters of the flat burnishing process are optimized to improve simultaneously the power factor, energy consumption, surface roughness, and

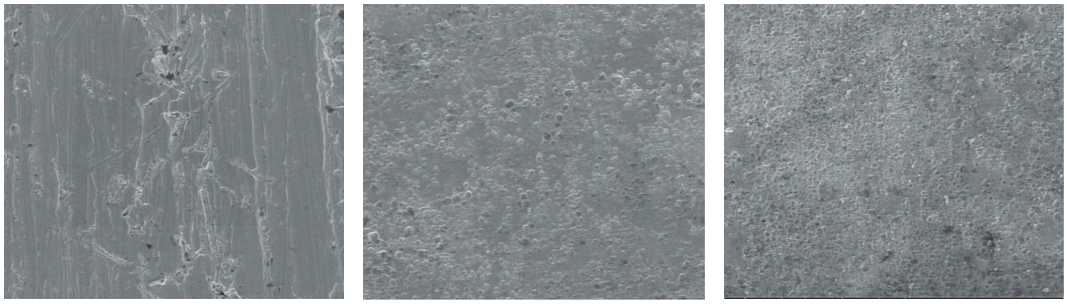

(a) Milled surface

(b) Surface at the V = 1000 (RPM), f = 200 (mm/min), and d = 0.10 (mm)

(c) Surface at the V = 1000 (RPM), f = 500 (mm/min), and d = 0.04 (mm)

Figure 15. Surface morphology at the difrerent conditions.

Table 7. Normalized results.

No.	PFB	ECB	K_{Ra}	K_{BH}
1	0.207106093	0.329312944	0.260039261	0.037933935
2	0.219547175	0.209711248	0.250800031	0.120691420
3	0.243091668	0.161870569	0.235852127	0.195444132
4	0.274490822	0.136028918	0.233189336	0.360949529
5	0.220667994	0.366586405	0.264891779	0.095519670
6	0.221869218	0.209615182	0.246108586	0.148225773
7	0.268656070	0.177721396	0.273511384	0.324628914
8	0.269530796	0.136509246	0.241465028	0.294972802
9	0.238791137	0.402611012	0.283512448	0.186493795
10	0.263234721	0.252940777	0.290827503	0.303816280
11	0.240440689	0.161774504	0.225636299	0.207595770
12	0.264232899	0.136509246	0.213314907	0.279590088
13	0.264724272	0.437290701	0.278172356	0.310856310
14	0.260761611	0.250539136	0.256000816	0.241195860
15	0.262509438	0.175992215	0.218253041	0.271315144
16	0.266069254	0.135932852	0.209042834	0.339490751

Table 8. Eigenvalues and proportions of principal components.

Principal component	Eigen values	Proportion (%)
First	3.0009	75.00
Second	0.9408	23.50
Third	0.0436	1.10
Fourth	0.0148	0.40

Table 9. Eigenvectors and contributions for the principal components.

	Eigenvectors				
Quality Characteristics	PC1	PC2	PC3	PC4	Contribution
PFB	−0.546	0.440	0.124	0.702	0.25
EFB	0.496	0.459	0.737	−0.032	0.23
K_{Ra}	0.390	0.641	−0.661	0.020	0.28
K_{BH}	−0.551	0.431	0.072	−0.711	0.24

Table 10. Normalized weighted values.

No.	PFB	ECB	K_{Ra}	K_{BH}
1	0.051776523	0.075741977	0.072810993	0.009104144
2	0.054886794	0.048233587	0.070224009	0.028965941
3	0.060772917	0.037230231	0.066038596	0.046906592
4	0.068622706	0.031286651	0.065293014	0.086627887
5	0.055166998	0.084314873	0.074169698	0.022924721
6	0.055467305	0.048211492	0.068910404	0.035574186
7	0.067164017	0.040875921	0.076583188	0.077910939
8	0.067382699	0.031397126	0.067610208	0.070793472
9	0.059697784	0.092600533	0.079383485	0.044758511
10	0.065808680	0.058176379	0.081431701	0.072915907
11	0.060110172	0.037208136	0.063178164	0.049822985
12	0.066058225	0.031397126	0.059728174	0.067101621
13	0.066181068	0.100576861	0.077888260	0.074605514
14	0.065190403	0.057624001	0.071680229	0.057887006
15	0.065627359	0.040478210	0.061110852	0.065115635
16	0.066517313	0.031264556	0.058531993	0.081477780

Table 11. MPI values and ranking.

No.	D^+	D^-	D	Ranking
1	0.091357989	0.0318068	0.258245613	15
2	0.062666863	0.0540619	0.463141320	12
3	0.043725707	0.0687402	0.611209096	9
4	0.016138702	0.0958579	0.855900039	3
5	0.084298412	0.0228141	0.212992284	16
6	0.056776108	0.0549861	0.491992010	11
7	0.013928366	0.0845595	0.858577833	**1**
8	0.021055108	0.0860420	0.803401651	2
9	0.074826440	0.0322159	0.300964397	14
10	0.030334524	0.0708394	0.700174420	7
11	0.042374306	0.0694993	0.621230433	8
12	0.029307205	0.0833237	0.739794189	5
13	0.070478725	0.0570356	0.447287812	13
14	0.040345142	0.0584818	0.591759575	10
15	0.031138038	0.0747691	0.705987333	6
16	0.023565927	0.0919236	0.795947489	4

Brinell hardness. This work has been considered not only the technical responses in terms of the machined part quality (roughness and hardness) but also environmental influences and sustainable machining objectives (energy consumption and power factor). A specific implementation of the flat burnishing process of SKD61 steel was successfully conducted to obtain the optimal factors for simultaneous improvements in the power factor, energy consumption, surface roughness, and Brinell hardness. The results obtained can be used in knowledge-based systems for industrial applications of the burnishing process. This paper is aimed to fulfill the academic gaps in scientific knowledge of the flat burnishing process. Moreover, the outcomes can be considered as technical solutions for improvements in energy efficiency and surface quality of the burnishing operation.

Conclusions

An optimization for the flat burnishing process of SKD61 steel has been presented in order to enhance energy efficiency and surface properties. The objectives are the power factor,

Table 12. Optimization results using Taguchi-PCA-TOPSIS.

	Optimization parameters			Responses					
Method	*V* RPM	*f* mm/min	*d* mm	PFB	ECB kJ	R_{aB} μm	K_{Ra}	ABH_B HB	K_{BH}
The worst case	700	200	0.07	0.679	42.00	0.29	0.80	332	0.30
Taguchi-GRA-TOPSIS	700	500	0.13	0.827	21.22	0.25	0.82	518	1.03
Improvement(%)				21.80	49.48	13.79	2.50	56.02	243.33

energy consumption, the reduction of the average roughness, and the improvement in the Brinell hardness. The processing factors optimized are the burnishing speed, feed, and depth of penetration. The PCA was applied to calculate the weight objectives. An optimizing technique entitled TOPSIS was applied to achieve a setting of optimal value. The resulting conclusions of this work can be listed as follows:

(1) It can be stated that the processing factors have significant impacts on the technical outputs. The maximal levels of the inputs are recommended to increase the power factor and the Brinell hardness. The highest value of the *d* has a significant contribution on a smoother surface, while the low levels of the *V* and *f* lead to a decrease in the roughness. The maximal levels of the spindle speed and the feed rate are recommended to save energy consumption. The minimal value of the depth of penetration is used to decrease energy used.
(2) The optimal values of the *V*, *f*, and *d* are 700 RPM, 500 mm/min, and 0.13 mm, respectively. The power factor is improved by 21.80% and the energy consumption is declined by 49.48%, respectively, as compared to the worst case. The reduction of the average roughness and the improvement of the Brinell hardness are increased by 2.50% and 243.33%, respectively. The burnishing process has effective impacts on the improvement of the surface characteristics. The average roughness can reduce approximately 82.52% and the Brinell hardness improves about 103.14%, as compared to the milled state.
(3) The application of a hybrid approach using Taguchi, PCA, and TOPSIS is an intelligent solution in order to save the experimental costs and ensure the reliable as well as feasible optimizing values, as compared to the practical experience or operation guide.
(4) Practically, the variation of the inputs may lead to contradictory impacts on the technical responses. A comprehensive optimization should be considered with more responses, such as the burnishing costs, residual stress, and productivity.

Declaration of conflicting interests

The author(s) declared no potential conflicts of interest with respect to the research, authorship, and/or publication of this article.

Funding

This research is funded by Vietnam National Foundation for Science and Technology Development (NAFOSTED) under grant number [107.04-2017.06].

ORCID

Trung-Thanh Nguyen http://orcid.org/0000-0002-0838-872X

References

[1] El-Taweel, T. A.; Ebeid, S. J. Effect of Hybrid Electrochemical Smoothing-roller Burnishing Process Parameters on Roundness Error and Micro-hardness. *Int. J. Adv. Manuf.Technol.* 2009, *42* (7), 643–655. DOI: 10.1007/s00170-008-1632-0.
[2] Stalin John, R.; Vinayagam, B. K. Optimization of Ball Burnishing Process on Tool Steel (T215cr12) in Cnc Machining Centre Using Response Surface Methodology. *A. J. S. E. Eng.* 2011, *36*(7), 1407–1422. DOI: 10.1007/s13369-011-0126-9.
[3] Travieso-Rodríguez, J. A.; Dessein, G.; González-Rojas, H. A. Improving the Surface Finish of Concave and Convex Surfaces Using a Ball Burnishing Process. *Mater. Manuf. Process.* 2011, *26* (12), 1494–1502. DOI: 10.1080/10426914.2010.544819.
[4] Ravindra Babu, P.; Ankamma, K.; Siva Prasad, T.; Raju, N.; Eswara Prasad, A. V. S. Optimization of Burnishing Parameters and Determination of Select Surface Characteristics in Engineering Materials. *Sadhana*. 2012, *37*(4), 503–520. DOI: 10.1007/s12046-012-0092-2.
[5] Revankar, G. D.; Shetty, R.; Rao, S. S.; Gaitonde, V. N. Analysis of Surface Roughness and Hardness in Ball Burnishing of Titanium Alloy. *Measurement*. 2014, *58*, 256–268. DOI: 10.1016/j.measurement.2014.08.043.
[6] Hamadache, H.; Zemouri, Z.; Laouar, L.; Dominiak, S. Improvement of Surface Conditions of 36 Cr Ni Mo 6 Steel by Ball Burnishing Process. *J. Mech. Sci. Technol.* 2014, *28*(4), 1491–1498. DOI: 10.1007/s12206-014-0135-1.
[7] Cobanoglu, T.; Ozturk, S. Effect of Burnishing Parameters on the Surface Quality and Hardness. *Proc. Inst. Mech. Eng. B.* 2015, *229* (2), 286–294. DOI: 10.1177/0954405414527962.
[8] Gharbi, F.; Sghaier, S.; Morel, F. Experimental Investigation of the Effect of Burnishing Force on Service Properties of AISI 1010 Steel Plates. *J. Mater. Eng. Perform.* 2015, *24*(2), 721–725. DOI: 10.1007/s11665-014-1349-1.
[9] Banh, Q. N.; Shiou, F. J. Determination of Optimal Small Ball-burnishing Parameters for Both Surface Roughness and Superficial Hardness Improvement of Stavax. *A. J. S. E. Eng.* 2016, *41*(2), 639–652. DOI: 10.1007/s13369-015-1710-1.
[10] Yuan, X. L.; Sun, Y. W.; Gao, L. S.; Jiang, S. L. Effect of Roller Burnishing Process Parameters on the Surface Roughness and Microhardness for TA2 Alloy. *Int. J. Adv. Manuf.Technol.* 2016, *85*(5–8), 1373–1383. DOI: 10.1007/s00170-015-8031-0.
[11] Stalin John, M. R.; Banerjee, N.; Shrivastava, K.; Vinayagam, B. K. Optimization of Roller Burnishing Process on EN-9 Grade Alloy Steel Using Response Surface Methodology. *J. Braz. Soc. Mech. Sci.* 2017, *39*(8), 3089–3101. DOI: 10.1007/s40430-016-0674-8.
[12] Stalin John, M. R.; Balaji, B.; Vinayagam, B. K. Optimisation of Internal Roller Burnishing Process in CNC Machining Center Using Response Surface Methodology. *J. Braz. Soc. Mech. Sci.* 2017, *39*(10), 4045–4057. DOI: 10.1007/s40430-017-0871-0.
[13] Robles, A. S.; Mora, H. P.; Gómez, E. A.; Robles, A. S.; Herrera, A. M.; De la Peña, J. A. D. Influence of Ball-burnishing on Roughness, Hardness and Corrosion Resistance of AISI 1045 Steel. *Surf. Coat. Tech.* 2018, *339*, 191–198. DOI: 10.1016/j.surfcoat.2018.02.013.

[14] Nguyen, T. T.; Le, X. B. Optimization of Interior Roller Burnishing Process for Improving Surface Quality. *Mater. Manuf. Process.* 2018, *33*(11), 1233–1241. DOI: 10.1080/10426914.2018.1453159.

[15] Nguyen, T. T.; Le, X. B. Optimization of Roller Burnishing Process Using Kriging Model to Improve Surface Properties. *Proc. Inst. Mech. Eng. B.* 2019, *233*(12), 2264–2282. DOI: 10.1177/0954405419835295.

[16] Sachin, B.; Narendranath, S.; Chakradhar, D. Selection of Optimal Process Parameters in Sustainable Diamond Burnishing of 17-4 PH Stainless Steel. *Braz. Soc. Mech. Sci.* 2019. DOI: 10.1007/s40430-019-1726-7.

[17] Świrad, S.; Wydrzynski, D.; Nieslony, P.; Krolczyk, G. M. Influence of Hydrostatic Burnishing Strategy on the Surface Topography of Martensitic Steel. *Measurement*. 2019, *138*, 590–601. DOI: 10.1016/j.measurement.2019.02.081.

[18] Huuki, J.; Laakso, S. V. A. Integrity of Surfaces Finished with Ultrasonic Burnishing. *Proc. Inst. Mech. Eng. B.* 2012, *227*(1), 45–53. DOI: 10.1177/0954405412462805.

[19] Amini, S.; Bagheri, A.; Teimouri, R. Ultrasonic-assisted Ball Burnishing of Aluminum 6061 and AISI 1045 Steel. *Mater. Manuf. Process.* 2018, *33*(11), 1250–1259. DOI: 10.1080/10426914.2017.1364862.

[20] Ishfaq, K.; Ahmed, N.; Hamza, H.; Zahid, M.; Al-Ahmari, A. Significant Improvement in Cutting Rate during WEDM of Clad-composite Using Zinc-coated Wire. *Mater. Manuf. Process.* 2019. DOI: 10.1080/10426914.2019.1669801.

[21] Arunramnath, R.; Thyla, P. R.; Mahendrakumar, N.; Ramesh, M.; Siddeshwaran, A. Multi-attribute Optimization of End Milling Epoxy Granite Composites Using TOPSIS. *Mater. Manuf. Process.* 2019, *34*(5), 530–543. DOI: 10.1080/10426914.2019.1566960.

[22] Global Greenhouse Gas Emissions Data. https://www.epa.gov (accessed October 26, 2019).

[23] Global Energy & CO2 Status Report 2018. https://webstore.iea.org (accessed October 26, 2019).

[24] International energy outlook 2017. https://www.eia.gov (accessed October 26, 2019).